

## Vertical load tests on zero sheet pile pressed-in into alluvial soft ground

Y. Toda

*Scientific Research Section, GIKEN LTD., Kochi, Japan*

M. Eguchi

*Assistant Manager, Scientific Research Section, GIKEN LTD., Kochi, Japan*

A. Mori

*Chief, Scientific Research Section, GIKEN LTD., Kochi, Japan*

Y. Ishihara

*Manager, Scientific Research Section, GIKEN LTD., Kochi, Japan*

### ABSTRACT

Steel sheet piles are primarily used for temporary structures, including cofferdams and shoring. They are also utilized for non-temporary structures such as revetments and retaining walls. Steel sheet piles come in various types with different cross-sectional shapes and dimensions. The "Zero sheet pile" discussed in this paper is one of them. Since the primary usage scenarios for zero sheet piles and the other steel sheet piles have been in horizontal loading, there are currently limited examples of vertical load testing on zero sheet piles. This paper reports on vertical load tests conducted in two cases with the purpose of obtaining data on the vertical bearing capacity characteristics of pressed-in zero sheet piles. The first case involved a sheet pile wall consisting of three interconnected sheet piles (Case1), while the second case utilized single sheet piles (Case2). In both cases, the piles were statically installed by Standard Press-in method (without the use of penetration assistance such as water jet or auger). In analysing the results, the second limit resistance was defined as the maximum pile head load reached until the pile head settlement reaches 0.1 times the pile diameter ( $D_o$ ), with  $D_o$  being the outer diameter of an equivalent steel pipe pile having the same cross-sectional area (both the tip and inner hollow section) as that of the zero sheet pile. For Case2, the load-displacement curve was extrapolated using Weibull Approximation method to cope with the accidental cease of the load test before the second limit resistance was attained. As a result, the second limit resistance for Case1 and Case2 were 1022 kN and 308 kN respectively.

**Key words:** *Steel sheet pile, load test, Vertical capacity, Standard press-in*

### 1. Introduction

Among various types of steel sheet piles, zero sheet piles are distinguished by their capability to facilitate construction proximate to existing structures together with the utilization of specialized press-in machines, as exemplified in **Figure 1**. Presently, zero sheet piles are employed predominantly as temporary structures, akin to other steel sheet piles, to provide horizontal resistance,

such as in retaining walls, which consequently results in a scarcity of instances where vertical load tests are conducted on them. However, the non-temporary applications of steel sheet piles have been gradually increasing in recent times. For instance, GIKEN RED HILL1967 (**Figure 2**), which opened to the public in May 2023, features zero sheet piles as the foundation for Sozokan (The Museum of Piling Machines) and

Research Building (Kondo *et al.*, 2022; Kondo *et al.*, 2023; Kondo *et al.*, 2024). In the pursuit of expanding the applications of steel sheet piles, including zero sheet piles, particularly as components expected to provide vertical resistance, it is imperative to accumulate data regarding their vertical bearing capacity characteristics. This paper reports results from vertical load tests on zero sheet piles in alluvial soft ground.



Fig.1 Example of installation of Zero Sheet Piles. (<https://www.giken.com/ja/solution/zero/>)



Fig.2 RED HILL 1967 (<https://redhill1967.giken.com/about/>)

## 2. Method of field test

### 2.1. Test piles and test case

The piles utilized in the experiment were zero sheet piles (SM-J295), each with a length of 6.4 meters. We conducted loading tests in two distinct cases. Case1 involved an assembly of three interlocked zero sheet piles, whereas Case2 utilized a single pile. All piles were installed using the Standard Press-in method, a technique that forgoes auxiliary penetration methods such as water jetting or augering. For Case2, we affixed strain gauges on the back side of the sheet pile to measure the distribution of axial strain. These gauges were protected

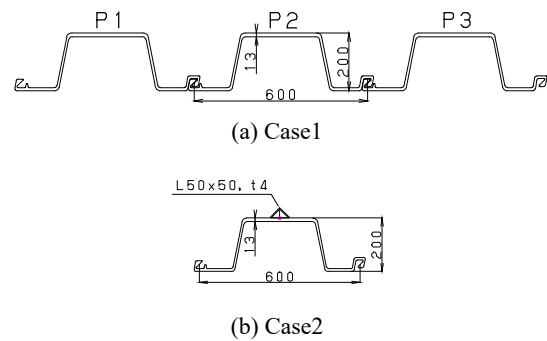


Fig.3 Piles cross-section (unit : mm)

with equilateral angle steel (50 mm by 50 mm with a 4 mm thickness and 6000 mm in length). **Figure 3** shows cross-sectional details of the piles used in each case.

### 2.2. Ground condition and test layout

We conducted the field test within a site owned by GIKEN. **Figure 4** shows the test layout and the ground conditions at the site. The ground is composed of a silt layer with a maximum  $N$ -value of 22 up to a depth of 3.5 m, beneath which lies a stratum of clay and ashy materials with  $N$ -values less than 10. However, prior to penetration of the zero sheet piles, we excavated the ground to a depth of approximately 4 meters, compacting and backfilling the excavated area (**Figure 5**). This process was undertaken to remove the surface gravel, facilitating penetration of the zero sheet piles using the Standard Press-in Method. We additionally performed a screw weight sounding test (SWS) to investigate the ground condition of the excavated area. Observing the converted  $N$  values obtained from SWS in **Figure 4**, they are broadly consistent with the original ground conditions. It is important to note, however, that the ground curing period after the compacting and backfilling processes was longer for the SWS than for the load test by 24 days. Exceptionally, a sharp increase in Converted  $N$  values was observed around depths of 2.7 m and 5 m, likely due to the screw point coming into contact with gravel that was not fully removed.

### 2.3. Method of Press-in piling

As mentioned in Section 2.1, we used the Standard Press-in Method for pile installation. The conditions of press-in piling are presented in **Table 1**. To monitor the jacking force and penetration depth chronologically

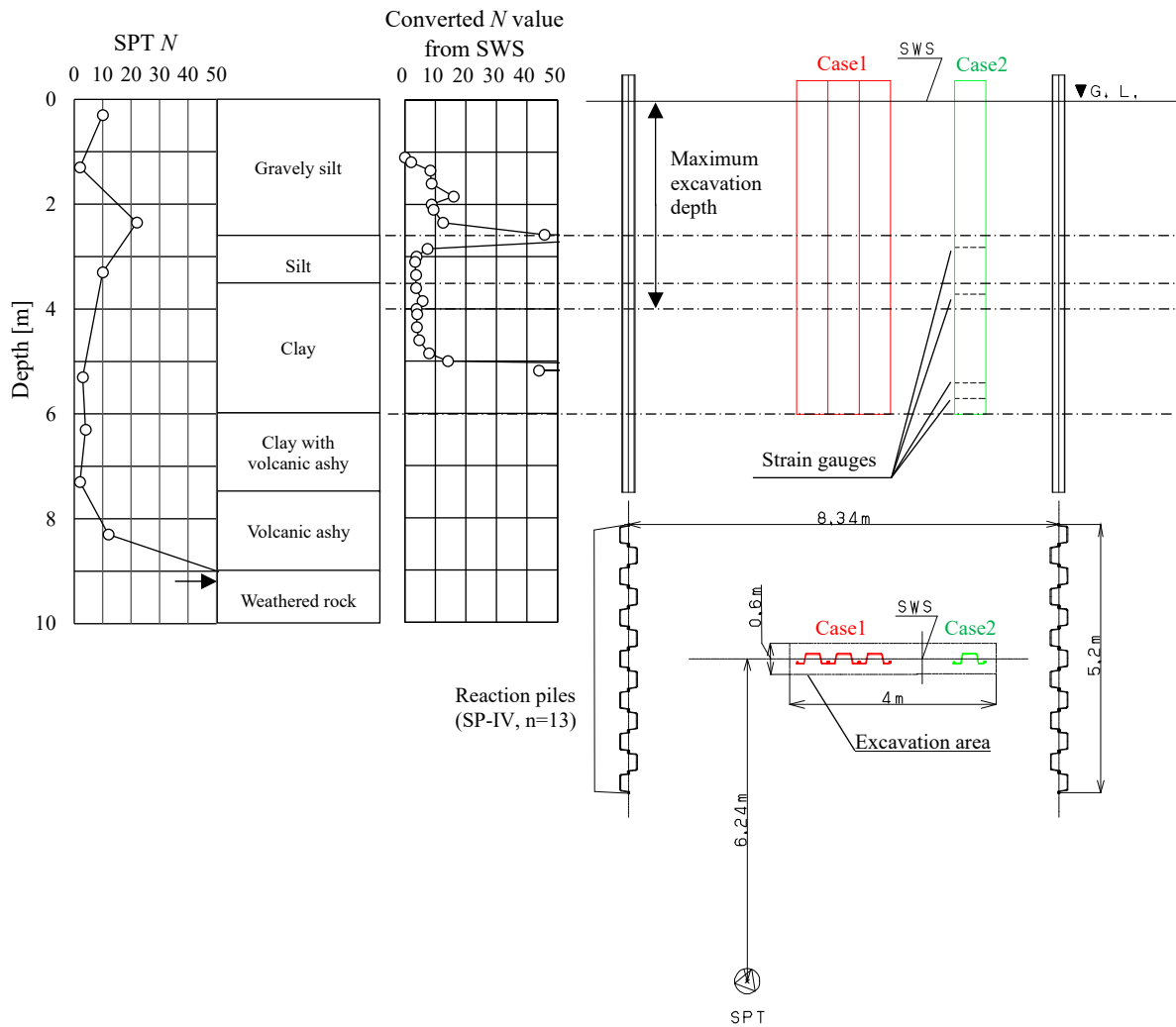


Fig.4 Ground condition and test layout.



Fig.5 Situation of excavation

Table.1 Conditions of press-in piling

	$z$	$Q'_{UL}$	$v_d$	$v_u$	$l_d (l_u)$
	[m]	[kN]	[mm/s]	[mm/s]	[mm]
Case1 (P1~P3)	$z \leq 2$	300	270	120	Arbitrary (manual)
	$2 < z \leq 5$	300	270	120	200 (100)
Case2	$5 < z$	400	180 -270	120	Arbitrary (manual)
	$5.97 \leq z \leq 6$	-	80	-	Arbitrary (manual)

$z$  : Penetration depth

$Q'_{UL}$  : Manually-set upper-limit of jacking force  $Q'$

$v_d$  : Penetration velocity in each cycle of surging

$v_u$  : Extraction velocity in each cycle of surging

$l_d$  : Displacement of penetration in each cycle of surging

during penetration, we equipped the press-in machine with a hydraulic sensor and the pile head with a stroke sensor. Throughout the penetration, we continuously applied water to the pile that shaft at the ground surface to prevent plugs, maintaining a flow rate of 12 L/min. **Figure 6** shows the situation of press-in piling in Case1.



**Fig.6** Situation of press-in piling of zero sheet piles. Wire end was connected to the pile head.

**2.4. Method of Loading tests**

We conducted the loading test based on the JGS Standard (JGS, 2002), as shown in **Figure 7**. The loading methodology employed was a combination of the continuous loading method and the single-cycle method. The curing period from the completion of installation to the loading test was 28 days for both cases.

The reaction force was secured using reaction piles (SP-IV, 8 m in length, 13 sheets × 2 lanes) and a beam, which were coupled using a newly developed clamping device (**Figure 8**). In terms of the loading equipment, for Case1, we used two hydraulic jacks, each with a maximum load capacity of 2 MN. For Case2, a single jack with a maximum load capacity of 1 MN was used. As shown in **Figure 9**, hydraulic jacks were set on top of the plate placed on the pile head.

The measured parameters included the pile head load, vertical and horizontal displacement of the pile head, and vertical displacement of the reaction piles.

**3. Results of field tests**

**3.1. Results of Press-in pilling**

**Figure 10** shows the penetration results, illustrating the relationship between penetration depth and pile head load  $Q$ .  $Q$  is provided by **Eq. (1)**, (Ishihara *et al.*, 2020).

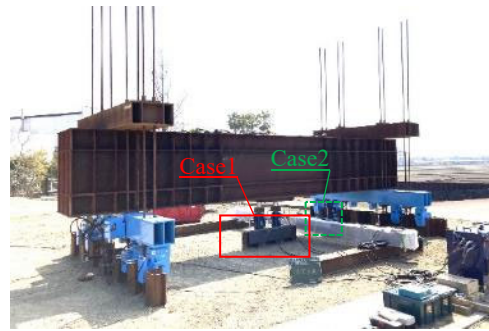


**Fig.7** Situation of load test of Case1

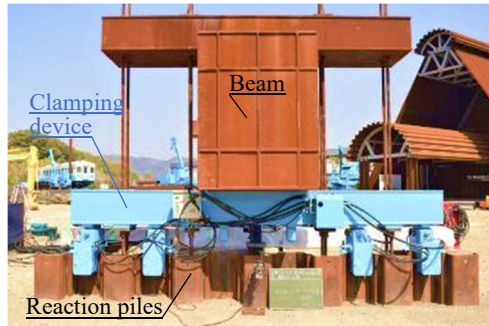


**Fig.8** Coupling of a beam and reaction piles using a clamping device.

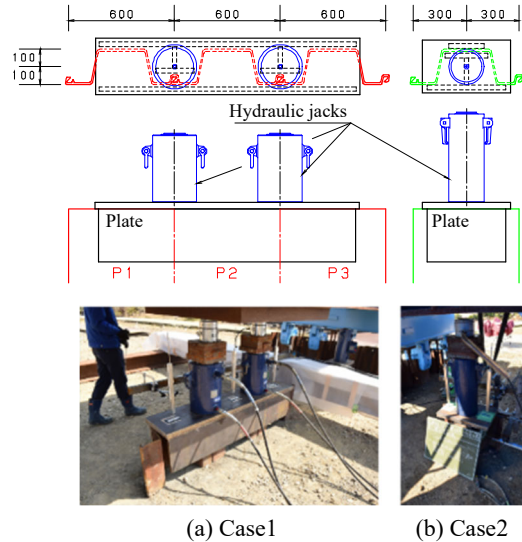


**Fig.9** The pile head condition during the loading test. In both cases, the plates and piles were not fixed, the plates were simply placed.

**Table.2** Load test conditions

	Number of piles	Curing period	Method for Load test
	-	day	-
Case1	3, With interlock connection	28	Continues, Single cycle
Case2	1	28	Continues, Single cycle

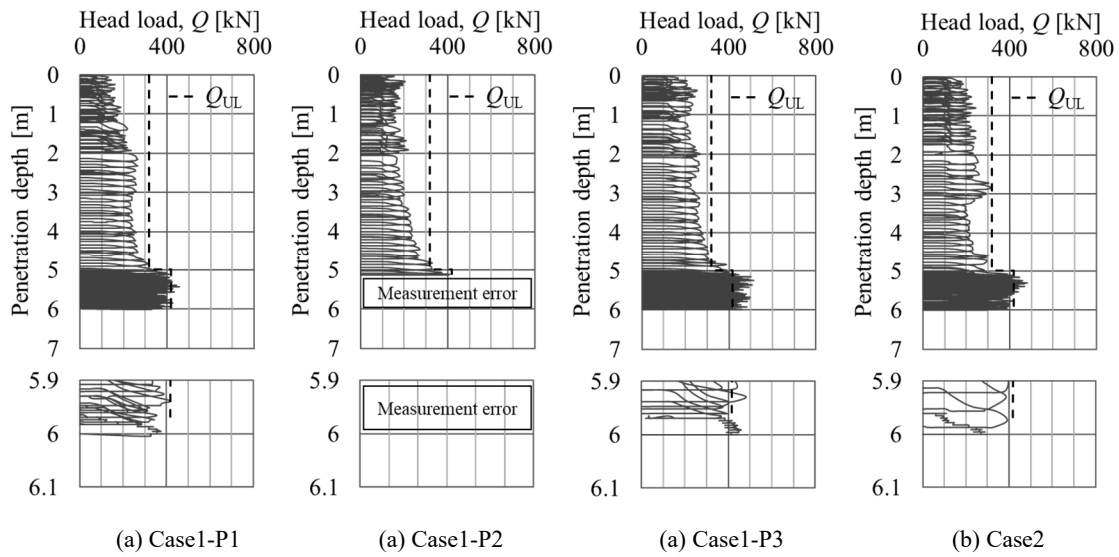


**Fig.10** Results of press-in piling. (a) is case1, (b) is case2. Case1-P2 has no data after 5 m depth of penetration due to measurement error.

$$Q = Q' + W_c \quad (1)$$

Where,  $Q'$  is the jacking force calculated from the hydraulic sensor affixed to the press-in machine.  $W_c$  is the weight of the chuck on the press-in machine, which was 18 kN for this test. Within **Figure 10**,  $Q_{UL}$  indicates the upper limit of the pile head load during penetration. We conducted the penetration in Case1 in the sequence of P1, P2, and P3. Due to a measurement error in the stroke sensor, no data beyond 5 m depth was available for P2. The graphs demonstrate good reproducibility in the relationship between penetration depth and pile head load, confirming consistent press-in under identical conditions. Beyond a penetration depth of 3 m, the head load slightly differed, with  $P1 < P3$ . From around 5 m depth, P3's head load consistently reached the upper limit,  $Q_{UL}$ . The lower graph in **Figure 10** magnifies the range between 5.9 m and 6.1 m of penetration depth. Within this depth interval, the head load was slightly smaller in P1 than in P3, with P3's head load reaching  $Q_{UL}$ . This is thought to be attributed to the influence of increased stress within the ground from the continuous penetration from P1 to P3, along with the resistance between joints. In fact, the single pile in Case2 was penetrated with a head load nearly identical to P1 across all depth ranges.

### 3.2. Results of Loading test

**Figure 11** shows the relationship between pile head load and vertical displacement obtained from the loading

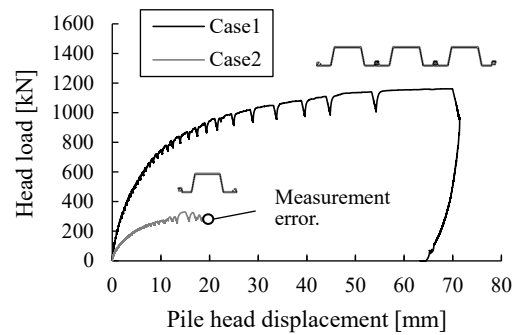


**Fig.11** Load-displacement curves.

tests. In Case1, the load-displacement curve almost paralleled the horizontal axis, indicating that the load was applied until the pile head load stabilized. For Case2, due to measurement errors, there was no data available for pile head displacements beyond 19 mm. Nonetheless, the load-displacement curve clearly shifted to a yielding phase.

**Figure 12** shows the relationship between axial force and pile head displacement at various sections of Case2. It should be noted that the initial value of axial force was taken from the measurements just before the loading test, disregarding the axial force generated in the pile during penetration. Considering the axial force 0.3m above the pile tip as the base resistance, it began to yield at the same displacement (pile head displacement  $\approx 5$  mm) as the other sections. Thereafter, despite an increase in head load, it remained in almost constant. This is thought to be attributed to the short length of the test pile,

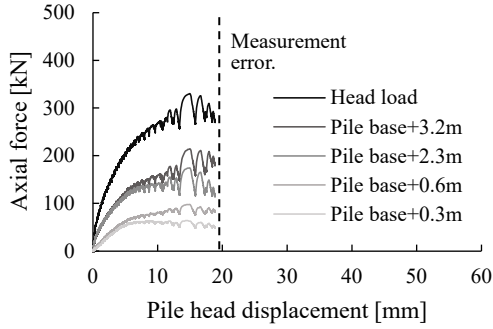


Fig.12 Axial force-displacement curves in Case2.

6.4 m, which facilitated the transmission of pile head load to the pile tip, and the fact that the pile tip was not embedded in hard ground, resulting in limited increase in base resistance.

Figure 13 shows the distribution of axial force at various load stages for Case2. The axial force at the section 0 m from the pile head corresponds to the value of the pile head load. From the distribution of axial forces, it is observed that the frictional resistance in sections A, C, and D increased progressively with each loading stage. On the other hand, the frictional resistance in section B remained approximately 0 kN until the pile head load reached about 150 kN. Thereafter, it gradually increased as the loading stages progressed. This is thought to be due to the progression of plugs in this section as the pile head displacement increased.

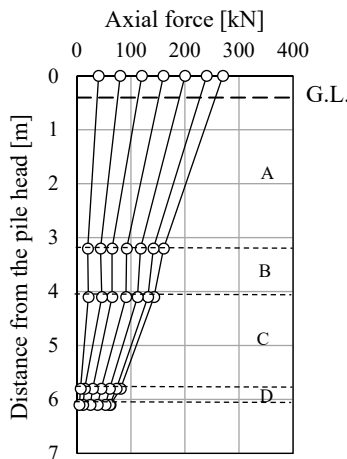


Fig.13 Distribution of axial forces in Case2

For Case2, we extrapolated using the Weibull distribution (Eq. (2)), referencing Uto *et al.* (1982). This approach was necessitated by the inability to load until the pile head displacement reached the displacement defining the bearing capacity, due to the reasons

mentioned earlier.

$$P = P_{\max} \times \left\{ 1 - e^{-\left(\frac{S}{S_0}\right)^m} \right\} \quad (2)$$

Where,  $P$  is the load,  $P_{\max}$  is the ultimate bearing capacity,  $S$  is the pile head displacement,  $S_0$  is the pile head displacement corresponding to the yield load, and  $m$  is the displacement index.

#### 4. Comparison of Case1 and Case2

Figure 14 shows the load-displacement curve for Case2 after extrapolation using the Weibull distribution. Table 3 lists the values of the first-limit-resistance and second-limit-resistance for each case. The values in parentheses represent the value per pile. We determined the first-limit-resistance from the log $P$ -log $S$  curve as instructed in the JGS Standard. On the other hand, the second-limit-resistance was defined as the maximum pile head load until the vertical displacement of the pile head reached 10% of the pile diameter. By the way, in the case of steel sheet piles, the geometric information corresponding to the pile diameter is not explicit. We used the method shown in Figure 15 to reinterpret the zero sheet piles as steel pipe piles and calculated the pile diameter. The converted pile diameter was  $D_o=293$  mm.

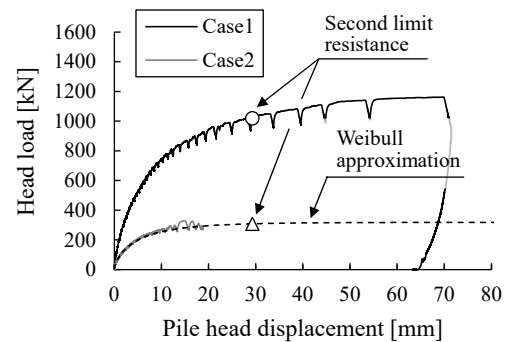


Fig.14 Comparison of load-displacement Case1 and Case2.

As can be observed from Table 3, for both Case1 and Case2, the value of the first-limit-resistance is approximately 75% of the second-limit-resistance.

When comparing the second-limit-resistance per pile, the value for Case1 was found to be approximately 1.1 times larger than that of Case2. It is generally understood that when piles are closely arranged, the vertical bearing capacity per pile tends to be lower than

**Table.3** Limit resistance

	Case1	Case2
	[kN]	[kN]
First-limit-resistance	746 (248)	238
Second-limit-resistance	1022 (340)	308

The first-limit-resistance was determined from the logP-logS curve. For Case 2, the second-limit-resistance value was estimated using the weibull approximation method.

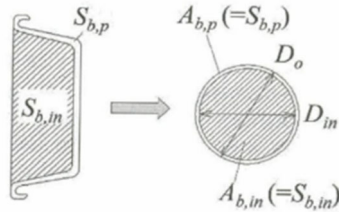


**Fig.15** Conversion to steel pipe pile. (IPA, 2017)

that expected for a single pile. This phenomenon, known as the pile group effect, is believed to arise from the overlap of vertical stresses transmitted to the ground from each pile due to the close spacing between them (JGS, 2020). On the other hand, Yetginer, *et al.* (2006) reported that in the cell foundations of pressed-in steel pipe piles, the pile group efficiency  $\eta$ , defined by Eq. (3), approached approximately 1.

$$\eta = \frac{Q_{2,Group}}{n \times Q_{2,Single}} \quad (3)$$

Where,  $Q_{2,Group}$  is second-limit-resistance of Group piles,  $Q_{2,Single}$  is second-limit-resistance of Single pile,  $n$  is number of piles. The reason posited is that the aforementioned pile group effect may have been offset by the increase in ground stress resulting from the continuous installation of the piles. In our test, the pile group efficiency  $\eta \approx 1.1$  was higher than the value of  $\eta \approx 1.0$  reported by Yetginer *et al.* (2006). This would be suggesting that the effect of increased stress within the ground due to the continuous installation of the zero sheet piles, offsetting the negative influence of the pile group effect, were greater than that of the pipe piles in the tests of Yetginer *et al.* (2006).

## 5. Conclusion

In this paper, we reported the results of vertical loading tests on zero sheet piles installed into alluvial soft ground by the Standard Press-in method. From these

results, we gained insights into the vertical bearing capacity performance as follows.

- The vertical resistance to the compressive load on zero sheet piles was predominantly provided by the frictional resistance. Furthermore, the increase in resistance after the friction reached a yield state was slight. The primary reason for these trends is believed to be the condition in which the zero sheet piles were not embedded into a bearing stratum.

- The second-limit-resistance per pile was greater for Case1 (with three interlocked piles) compared to Case2 (single pile). This is considered to be due to the effect of increased stress within the ground, resulting from continuous installation, being more significant than the pile group effect when a compressive load is applied to the zero sheet piles.

## References

- Kondo, Y., Sato, K., Nishimori, Y., Nakagawa, D. (2022) : Steel design, Sozokan [Tetsu no dezain, Sozokan]. *Tekko gijutsu*, Vol.35 (414), pp.37-43. (in Japanese)
- Kondo, Y., Sato, K., Nishimori, Y., Nakagawa, D. (2023) : Steel design, GIKEN Research Building [Tetsu no dezain, Gikenseisakusyo Kenkyuto]. *Tekko gijutsu*, Vol.36 (420), pp.32-41. (in Japanese)
- Kondo, Y., Sato, K., Nishimori, Y. (2024) : World's First Steel Sheet Pile-based Building Structures - Sozokan-. *Proceedings of the 3rd International Conference on Press-in Engineering 2024, Singapore*.
- Kondo, Y., Sato, K., Nishimori, Y. (2024) : World's First Steel Sheet Pile-based Building Structures -Research Building-, *Proceedings of the 3rd International Conference on Press-in Engineering 2024, Singapore*.
- The Japanese Geotechnical Society (JGS) (2002) : Method of static axial compressive load test of single piles, *Standards of Japanese Geotechnical Society for Vertical Load Tests of Piles*.
- Ishihara, Y., Ogawa, N., Mori, Y., Haigh, S. K., Matsumoto, T. (2020) : Simplified static vertical loading test on sheet piles using press-in piling machine, *8th Japan-China Geotechnical Symposium, Japanese Geotechnical Society Special Publication*, pp. 245-250.

Uto, K., Fuyuki, M., Sakurai, M. (1982) : Method for organizing the results of pile loading tests [Kui no saika shiken kekka no seiri hoho], *Foundation Engineering & Equipment, Monthly*, Vol.10 (9), pp.21-30. (in Japanese)

International Press-in Association (IPA) (2017) : Technical material on the use of piling data in the Press-in Method I . Estimation of subsurface information, pp.17

The Japanese Geotechnical Society (JGS) (2020) : Introduction to Foundation Bearing Capacity and Deformation [Kiso no sijiryoku to henkei nyumon], pp.130. (in Japanese)

Yetginer, A. G., White, D. J. & Bolton, M. D. (2006) : Field measurements of the stiffness of jacked piles and pile groups, *Geotechnique*, 56, No. 5, pp.349–354.